



Anti-hepatocellular carcinoma activity of *Sorbaria sorbifolia* by regulating VEGFR and c-Met/apoptotic pathway

Zhao-Hua Xu¹, Ying Dang¹, Yu Dong², Chong-Yang Dong², Yu Liu², Xu Chen², Zhi Yao², Jian-Ping Shi^{*}

College of Traditional Chinese Medicine, Inner Mongolia Medical College, Hohhot, China

ARTICLE INFO

Keywords:

Sorbaria sorbifolia
Hepatocellular carcinoma
Treatment
Apoptosis
Cancer-induced neovascularization
Signaling pathway

ABSTRACT

Ethnopharmacological relevance: *Sorbaria sorbifolia* (SS) is a traditional Chinese medicine (TCM) that has been employed anti-hepatocellular carcinoma (HCC) for over 2000 years; yet, its underlying mechanism is still not fully understood.

Aim of the study: In this study, we evaluated the anti-HCC effect on the freeze-dried powder of the water extract of SS (FDSS) by inhibiting tumor-induced neovascularization, and promoting apoptosis, and elucidated the underlying mechanisms.

Materials and methods: HCC cell lines (HepG2 and Huh7 cells) and HepG2 xenograft tumors in zebrafish were employed as in vivo and in vitro models, respectively, to evaluate the anti-HCC-induced neovascularization and apoptosis. In HCC cell lines, CCK-8 assay, wound-healing assay, transwell assay, cell circle assay, apoptosis assay, transmission electron microscopy, and co-culture assay were performed in vitro; in HepG2 xenograft tumor-zebrafish, tumor growth inhibition assay, hematoxylin and eosin (HE) staining, xenograft tumor-zebrafish apoptosis assay, and HCC-induced neovascularization assay were performed to evaluate the effect of FDSS on biological behavior of tumor, HCC-induced neovascularization, and apoptosis. The expression of VEGFR and c-Met/apoptotic pathway-related proteins was detected by western blotting analysis. Assays for c-Met and VEGFR activation were conducted to assess the impact of FDSS in either agonistic or inhibitory roles on these receptor proteins.

Results: The findings from our study revealed that FDSS effectively suppresses the proliferation, migration, and invasion of HepG2 and Huh7 cells, as well as inhibiting tumor growth in the HepG2 xenograft zebrafish model by downregulating the expression of p-Met and p-AKT proteins. FDSS decreased the tumor growth associated with promoting apoptosis, including arresting HepG2 and Huh7 cells cycle at G0/G1phase, increasing apoptotic cell numbers and apoptotic bodies in cancer cells, and increasing the apoptotic fluorescence of xenograft tumor zebrafish by downregulating Bcl-2 proteins and upregulating Bax, caspase-9, and caspase-3 levels. We also found that FDSS can inhibit HCC-induced neovascularization and regulate VEGFR. Using an agonist or inhibitor of c-Met and VEGFR in HepG2 cells, we discovered that FDSS can downregulate c-Met and VEGFR protein expression.

Conclusion: FDSS exerts an anti-HCC effect by inhibiting HCC-induced neovascularization and pro-apoptosis through the inhibition of the action of VEGFR and c-Met/apoptotic pathway.

1. Introduction

Primary liver cancer (PLC) is a common malignancy in China, accounting for 46.7% of PLC cases worldwide (Qiu et al., 2020). Over 90% of PLCs are hepatocellular carcinoma (HCC) (Siegel et al., 2019). In

China, the 5-year survival rate of HCC is only 12.1%, and morbidity and mortality of HCC rank fifth and third among all malignancies, respectively (Zeng et al., 2018). Despite the considerable advancement that has occurred in the treatment of HCC, the long-term outcomes are still not satisfactory, mainly due to the high recurrence rate (Wen et al.,

* Corresponding author.

E-mail addresses: r17604789390@163.com (Z.-H. Xu), dangying@163.com (Y. Dang), dongyu@163.com (Y. Dong), 150606915@qq.com (C.-Y. Dong), 150374930848@163.com (Y. Liu), 708813109@qq.com (X. Chen), 47370659@qq.com (Z. Yao), sjp4321@126.com (J.-P. Shi).

¹ Zhao-Hua Xu and Ying Dang are the first authors of this paper.

² These authors are the second authors of this paper.

<https://doi.org/10.1016/j.jep.2024.117758>

Received 21 October 2023; Received in revised form 2 December 2023; Accepted 11 January 2024

Available online 20 January 2024

0378-8741/© 2024 The Author(s). Published by Elsevier B.V. This is an open access article under the CC BY-NC-ND license (<http://creativecommons.org/licenses/by-nc-nd/4.0/>).

2022). Therefore, effective and safe new strategies are actively demanded.

TCM has been applied to treat cancer for thousands of years, because of its fewer side effects and certain efficacy. According to TCM theory, when blood is obstructed, it becomes condensed into “stasis,” referred to as tumors. Wang Qingren, a famous traditional Chinese doctor born in the Qing dynasty, reported that herbs which can activate blood and dissolve stasis have anticancer abilities (Shoja et al., 2010). Later on, many cases have supported the theory. For example, *Rhizoma Curcumae longae* (Liu et al., 2023), *Lobelia chinensis* Lour (Luo et al., 2024), Huaier granule (Wang et al., 2021) were used to treat hepatocellular carcinoma. Therefore, TCM herbs that activate blood and dissolve stasis have great potential for treating liver cancer.

Sorbaria sorbifolia (L.) A. Braun, a plant native to Changbai Mountain whose stem bark and spikes are used as medicine, has the ability to activate blood circulation and dissolve stasis (Liu et al., 2011). The name has been verified with “World Flora Online” (www.worldfloraonline.org). It has been used as an anti-tumor treatment for over 2000 years, as documented in the Dictionary of Anti-cancer Chinese Herbal Medicines (Zhang et al., 2004). The components of SS are mainly flavonoids, aromatic acids, lignans, and straws (Zhang et al., 2022) with anti-tumor (Zhang et al., 2007), anxiolytic (Mahnashi et al., 2023), anti-inflammatory (Jang et al., 2020), anti-photoaging (Jang et al., 2020), and hepatoprotective effects that may activate blood and dissolving stasis (College, 2006). Modern studies have reported that extracts of SS induce apoptosis in HepG-2 cells (Li et al., 2011), inhibit HCC growth in nude mice, and possess anti-tube formation properties in human umbilical vein endothelial cells (HUVECs) (Xiao et al., 2016). Nevertheless, its effect on inhibiting carcinoma-induced angiogenesis and apoptosis in animal models through regulating VEGFR and c-Met/apoptotic signaling pathways is still not fully understood.

Numerous studies have provided evidence that the abnormal activation of the c-Met signaling pathway amplifies the unfavorable biological characteristics of tumors. (Karmacharya et al., 2021). In HCC, the overexpression of c-Met is linked to the suppression of apoptosis and unfavorable clinical outcomes. (Wang et al., 2020). Tumors with a diameter >2 mm must acquire angiogenesis for further growth, which is usually induced by the expression of VEGFR (Jain, 2005). Preclinical studies have identified that strategy leads to upregulation of c-Met levels, suggesting that the two pathways synergistically promote tumor cell development and angiogenesis (Kummar et al., 2021). Thus, directly targeting VEGFR and c-Met/apoptotic pathway represents a potential therapeutic approach to treating HCC. Therefore, the hypothesis that SS exerts anti-HCC effects by regulating VEGFR and c-Met/apoptotic pathway was put forward. To verify this, a comprehensive series of in vitro and in vivo experiments were conducted to evaluate the tumor-inhibiting properties of SS on HCC cell lines and a xenograft model in larval zebrafish. Moreover, the roles of VEGFR and c-Met/apoptotic pathways during SS-treated HCC were further explored.

2. Materials and methods

2.1. Reagents and materials

SS was obtained from Huzhou Licensed Pharmaceutical Co., Ltd., (Haozhou, Anhui, China) Annexin-V: FITC apoptosis detection kit and cell cycle analysis kit were obtained from Servicebio (Wuhan, Hubei, China). Fetal bovine serum (FBS) and trypsin were purchased from Gibco (Grand Island, NY, USA). Cell counting kit-8, dimethyl sulfoxide (DMSO), and phosphate buffer saline (PBS) were obtained from Beyotime Biotechnology (Shanghai, China). Matrigel and transwell chambers were purchased from Corning Costar (Acton, MA, USA). Crystal violet staining solution, Sds-Page gel kit, and 4% tissue fix solution were obtained from Solarbio Life Science (Shanghai, China). Penicillin-streptomycin, CM-DiI cell-labeling, Roswell Park Memorial Institute (RPMI) 1640, formic acid, and acetonitrile were purchased from Thermo

Fisher Scientific (Waltham, MA, USA). Xylene, ethanol absolute, glutaraldehyde, osmium tetroxide, uranyl acetate, and lead citrate were obtained from Sinopharm Chemical Reagent Co., Ltd. (Shanghai, China). Hematoxylin dye solution and eosin stain solution were purchased from YIHE Biological (Shanghai, China). High-efficiency paraffin sections (melting points 54–56 °C) and high efficiency paraffin section (melting points 62–64 °C) were obtained from Shanghai Yonghua Paraffin Wax Co., Ltd., (Shanghai, China). Anti-caspase-3, anti-caspase-9, anti-Bcl-XL, anti-Bax, anti-phospho-Met, anti-phospho-AKT, anti-AKT, anti-VEGF, anti-β-actin, and anti-α-tubulin antibodies were purchased from Proteintech (Wuhan, Hubei, China). HY-132814, SU11274, HY-N0545, and sorafenib were obtained from MedChemExpress (Ravi, NJ, USA). Scutellarin, quercetin, kaempferol, ursolic acid, oleanolic acid, and chlorogenic acid were purchased from Chemical Book (Wuhan, Hubei, China).

2.2. Preparation of freeze-dried powder and the composition confirmation of the water extract of *Sorbaria sorbifolia* (SS)

2.2.1. Preparation of freeze-dried powder of SS

FDSS was isolated from 450 g of SS using water extraction, as Li's report (Li et al., 2013).

2.2.2. Component analysis of FDSS

Preparation of the test solution. 2 g of FDSS was taken, weighed accurately, and placed in a conical flask with a stopper. Then, 25 mL of 70% methanol was added accurately. Furthermore, the mixed system is subjected to ultrasound for 30 min before being colded down. Next, 70% methanol to reduce weight loss was supplied. Finally, the mixture was vigorously shaken and then filtered through a 0.22 μm filter membrane to obtain the solution for analysis.

Preparation of reference solution: Accurate measurements of Scutellarin, quercetin, kaempferol, ursolic acid, oleanolic acid, chlorogenic acid, and various other reference substances were precisely weighed and individually deposited into 25 mL volumetric flasks. Then, a small amount of methanol was added in volumetric flasks to dissolve the reference substance, and then methanol was added to the mark and shook well, and the reference solution was obtained.

Chromatographic conditions. A chromatographic column, specifically the ACQUITY UPLC HSS T3 C18 column (2.1 × 100 mm, 1.8 μm), was employed. The mobile phase consisted of a 0.1% formic acid aqueous solution (A) and a 0.1% formic acid acetonitrile solution (B). The conditions for recording chromatograms were gradient elution (0–1.08 min, 5%→5% B; 1.08–2.08 min, 5%→13.2% B; 2.08–6.08 min, 13.2%→13.5% B; 6.08–14.08 min, 13.5%→30% B; 14.08–20.08 min, 30%→41% B; 20.08–24.08 min, 41%→41% B; 24.08–28.08 min, 41%→57% B; 28.08–30 min, 57%→80% B; 30.08–32 min, 80%→90% B; 32–34 min, 90%→95% B), flow rate of 0.21 mL/min, column temperature of 40 °C and injection volume of 2 μL.

Mass spectrometry conditions. XEVO G2-XS ESI was applied as an ion source, and positive/negative ion mode was used. The cone hole voltage was set at 40 V, ion source temperature was set at 100 °C, the desolvent temperature was set 400 °C, the cone hole gas flow rate was set 50 L/h, desolvent gas flow rate was set 700 L/h. The scanning range was from m/z 100–1500, and leucine enkephalin ([M+H]⁺556.2771, [M-H]⁻554.2615) was applied as a calibration solution. Using Masslynx4.1 working software, mass spectrometry data was collected in MSE continuum mode with a scanning rate of 0.2/s and a collision energy of 20 V–35 V.

2.3. Cell experiments

2.3.1. Cell culture

HepG2, Huh7 cells, and HUVECs were sourced from the Chinese Cell Resource Center. These cells were maintained in RPMI 1640 basal medium with 10% FBS and 1% penicillin and streptomycin and cultivated

at 37 °C in a humidified environment consisting of 5% CO₂ and 95% air.

2.3.2. CCK-8 assay

HepG2 and Huh7 cells were diluted in 1640 complete medium, seeded at a density of 3×10^3 cells/100 μ L (100 μ L per well) in 96-well plates, and incubated for 24 or 48 h, then exposed to FDSS at concentrations of 20, 40, and 80 μ g/mL, in addition to 5 μ g/mL of sorafenib. Afterward, 10 μ L of CCK-8 solution was introduced to each well for a 1 h incubation. Absorbance readings were taken at 450 nm using an enzymatic labeler.

2.3.3. Transwell migration assay

The bottom wells of the chamber were filled with culture medium containing FDSS (20, 40, and 80 μ g/mL), and into the upper chamber, HepG2 and Huh7 cells (6×10^4 cells/well) were loaded. After 4 h, any non-migrated HepG2 and Huh7 cells were eliminated using a sterile cotton swab, followed by a triple wash with PBS. The cells were subsequently fixed with 4% paraformaldehyde, stained with 0.1% crystal violet for 20 min, photographed, and the number of migrating cells was quantified.

2.3.4. Wound healing assay

The HepG2 and Huh7 cells (6×10^4 cells/well) were seeded in 24-well culture plates. Once the cell monolayer reached confluence, it was gently scratched using a pipette tip, followed by two washes with PBS. Subsequently, the cells were exposed to FDSS (20, 40, and 80 μ g/mL) and sorafenib (5 μ g/mL) and incubated for 24 h. Images were captured at both 0 h and 24 h.

2.3.5. Cell cycle analysis

Following a 48-h exposure to FDSS (at concentrations of 20, 40, and 80 μ g/mL) and sorafenib (at 5 μ g/mL), the cells were collected, rinsed twice with pre-chilled PBS, stained in accordance with the guidelines provided by the Cell Cycle Detection Kit, and subsequently subjected to analysis using flow cytometry.

2.3.6. Apoptosis analysis

HepG2 and Huh7 cells (6×10^4 cells/well) were treated with FDSS (20, 40, and 80 μ g/mL) for 48 h, then harvested, washed with PBS, stained according to the instructions of the Annexin V-FITC/PI apoptosis detection kit, and analyzed by flow cytometry.

2.3.7. Transmission electron microscopy (TEM)

HepG2 and Huh7 cells (6×10^4 cells per well) were exposed to FDSS (at concentrations of 20, 40, and 80 μ g/mL) for 48 h. Subsequently, the cells were gathered in centrifuge tubes, washed twice with PBS, and then fixed with 2.5% glutaraldehyde for 90 min, followed by treatment with 1% osmium tetroxide for 30 min. The cells were then subjected to dehydration using a gradient of 95% anhydrous ethanol, embedding, sectioning, and staining with saturated uranyl acetate and lead citrate, followed by observation using TEM at a magnification of $8000 \times$.

2.3.8. Tumor cell-induced angiogenesis assay

HUVECs (1×10^5 cells per well) were plated on a surface coated with Matrigel (10 mg/mL) obtained from an angiogenesis kit. They were then exposed to conditioned medium collected from HepG2 and Huh7 cells (6×10^4 cells per well) treated with FDSS (at concentrations of 20, 40, and 80 μ g/mL) for 24 h. Subsequently, the cells were photographed using an optical microscope.

2.3.9. Western blot

Cell and xenograft tumor zebrafish tissue total protein extraction was carried out using RIPA with PMSF (in a 1:100 ratio) at 4 °C for 30 min and quantified using a BCA assay. Subsequently, 30 μ g of protein was separated via 8% SDS-PAGE and transferred to PVDF membranes. The membranes were first incubated with 5% non-fat milk for 30 min,

followed by exposure to primary antibodies, including AKT (1:1500), p-AKT (1:1000), Met (1:1000), p-Met (1:2000), Bcl-2 (1:2000), Bax (1:2000), caspase-9 (1:2000), caspase-3 (1:2000), VEGF (1:2000), and β -actin (1:2000), at room temperature for 1 h and then overnight at 37 °C. Subsequently, the membranes were washed and exposed to a secondary antibody, either anti-rabbit or anti-mouse, for 1 h at room temperature. The blots were visualized using Immobilon Western CHEMILUM HRP Substrate, and the chemiluminescent reactions were captured using X-ray film.

2.3.10. Inhibitor and agonist assay

HepG2 cells were inoculated into 96-well plates at 3×10^3 cells/100 μ L (100 μ L per well) and cultured for 24 h, after which they were treated in 4 different ways: (1) with HY-132814 (4 μ M) (c-Met agonist) and HY-132814 combined FDSS (20, 40, and 80 μ g/mL) after 48 h (2) with SU11274 (8 μ M) (c-Met inhibitor) and SU11274 combined FDSS (20, 40, and 80 μ g/mL). (3) with HY-N0545 (4 μ M) (VEGFR agonist) and HY-N0545 combined FDSS (20, 40, and 80 μ g/mL). (4) with sorafenib (4 μ g/mL) (VEGFR agonist) and sorafenib combined FDSS (20, 40, and 80 μ g/mL). The western Blot method was employed to investigate the expression of p-Met and VEGFR, following the protocol described in 2.3.9.

2.4. 4. Animal experiment

2.4.1. Zebrafish care and maintenance

Adult zebrafish were fed with live shrimp twice a day and housed in fish culture water at 28 °C. All animal studies were done in compliance with the regulations of Inner Mongolia Medical University institutional animal care (Laboratory animal's license number was No. SYXK (Zhe) 2022-000) and conducted according to the Association for Assessment and Accreditation of Laboratory Animal Care guidelines (certification number: 001458).

2.4.2. Growth and inhibition of HepG2 xenograft tumor

Adult zebrafish were provided with live shrimp as part of their diet twice daily and were accommodated in fish culture water maintained at a temperature of 28 °C. All animal-related investigations were conducted in adherence to the regulations established by Inner Mongolia Medical University's institutional animal care guidelines (Laboratory animal's license number: No. SYXK (Zhe) 2022-000) and in accordance with the principles outlined by the Association for Assessment and Accreditation of Laboratory Animal Care (certification number: 001458).

2.4.3. HE staining

Zebrafish xenograft tumors, treated with FDSS (at concentrations of 5, 10, and 20 μ g/mL) on the 5th day post-fertilization (5 dpf), underwent fixation with 4% paraformaldehyde at 4 °C overnight. After fixation, they were subjected to dehydration, clearing, embedding, and sectioning into 4 μ m slices for H&E staining. Subsequently, the samples were examined under a microscope.

2.4.4. Tumor-induced subintestinal vasopressor assay

HepG2 cells were transplanted by microinjection into the yolk sac of 2 dpf-Fli-1 strain zebrafish. At 3 dpf, xenograft tumor zebrafish were treated with FDSS and sorafenib. At 5 dpf, zebrafish were photographed under a Nikon A1R laser confocal microscope to observe intestine neo-vascularization buds.

2.4.5. Xenograft tumor zebrafish apoptotic assay

Xenograft tumor zebrafish were immersed in 2.5 μ g/mL acridine orange (AO) for 40 min and then rinsed four times with standard dilution water. Zebrafish were photographed under a fluorescence microscope. Data were acquired using NIS-Elements D 3.20 advanced image processing software to analyze the apoptotic fluorescence intensity of

tumor cells.

2.5. Statistical analysis

Statistical analysis was performed with the Student's t-test using SPSS 22.0 software. A p-value <0.05 represented a significant difference. All experiments were performed in triplicate.

3. Results

Under the experimental conditions in 2.2.2, the obtained ultrahigh-performance liquid chromatography diagram is shown in Fig. 1, and the characteristic components are shown in Table 1, which is consistent with the reference (Ying Zhang, 2021).

3.1. FDSS inhibited HCC cells growth, migration, and invasion ability of HCC cells in vitro

In the initial phase, we evaluated the impact of FDSS on the growth of HepG2 cells (Fig. 2A) and Huh7 cells (Fig. 2B). These cell lines were subjected to varying concentrations of FDSS (20, 40, and 80 µg/mL) as well as sorafenib (at 4 µg/mL) treatment over 24 and 48 h. The results revealed that FDSS led to a reduction in cell viability in both cell types, with the extent of inhibition correlating with the dose and duration of exposure. Notably, the growth-inhibiting effect of the FDSS (80 µg/mL) group was on par with that of the sorafenib group, which served as a positive control.

In order to assess the influence of FDSS on cell migration, we utilized wound closure assays. After a 24-h period (Fig. 2C), the healing rates for HepG2 cells treated with FDSS at concentrations of 20, 40, and 80 µg/mL, along with sorafenib at 4 µg/mL, were determined to be 75.2%, 59.3%, 41.8%, and 31.6%, respectively. Notably, the healing rates in all three treatment groups were significantly lower in comparison to the model control group (82.3%) (all $P < 0.01$). Furthermore, there were no significant differences observed between the FDSS (80 µg/mL) group and the sorafenib group ($P > 0.05$). Similarly, the healing rates for Huh7

Table 1

The characteristic components of SS.

Serial number	Retention time/min	Compound
1	4.76	Chlorogenic acid
2	11.88	Baicalin
3	14.78	Baicalin
4	16.98	Quercetin
5	19.57	Hanbaicalin
6	32.30	Oleanolic acid

cells exposed to FDSS at concentrations of 20, 40, and 80 µg/mL, as well as sorafenib at 4 µg/mL, were calculated as 60.6%, 45%, 28.6%, and 22.3%, respectively. These values exhibited a substantial decrease when compared to the model control group (77.3%) (all $P < 0.01$).

The transwell migration assay was subsequently utilized to evaluate the impact of FDSS on cell invasion. The quantity of HepG2 cells treated with FDSS at concentrations of 20, 40, and 80 µg/mL exhibited a noteworthy dose-dependent reduction when compared to the model control group ($P < 0.01$). A parallel outcome was observed for Huh7 cells (Fig. 2D).

These data suggest that FDSS inhibits the biological behavior of HCC cells in a dose-dependent manner.

3.2. FDSS inhibits HCC growth in vivo

In order to examine the effects of FDSS on the growth of tumors, we implanted HepG2 cells in zebrafish to establish a xenograft tumor model, then treated zebrafish with FDSS (5, 10, and 20 µg/mL) and sorafenib (0.134 µg/mL) (Fig. 3A). Compared with the model group, FDSS (10, 20 µg/mL) groups significantly inhibited the fluorescence of HepG2 cells ($P < 0.01$). In addition, the tumor fluorescence between the FDSS (10, 20 µg/mL) groups and the sorafenib group showed no significant difference ($P > 0.01$).

Next, HE staining was applied to observe cell structure in *ex vivo* (Fig. 3B). More tumor cells were pleomorphic with increased nucleoplasmic ratio (Rnp) in the model group, which indicated high invasion,

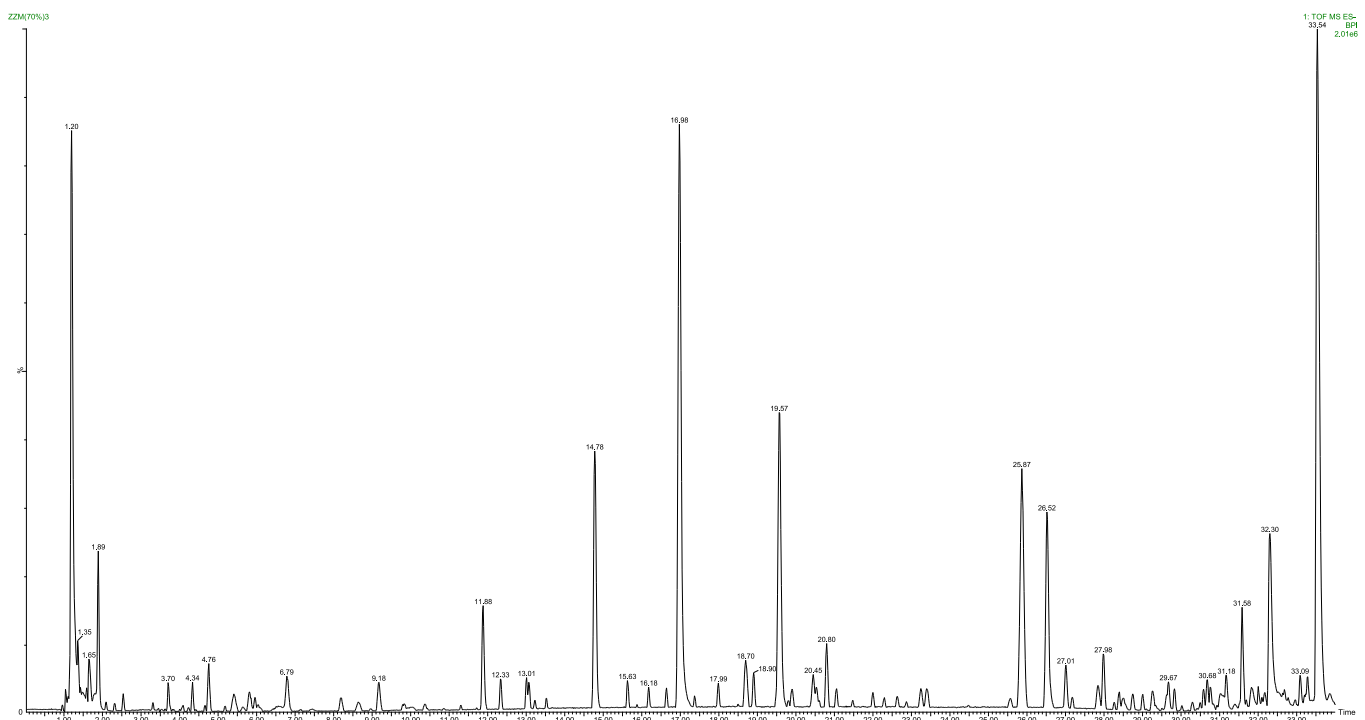


Fig. 1. The chromatography diagram of ultrahigh performance liquid.

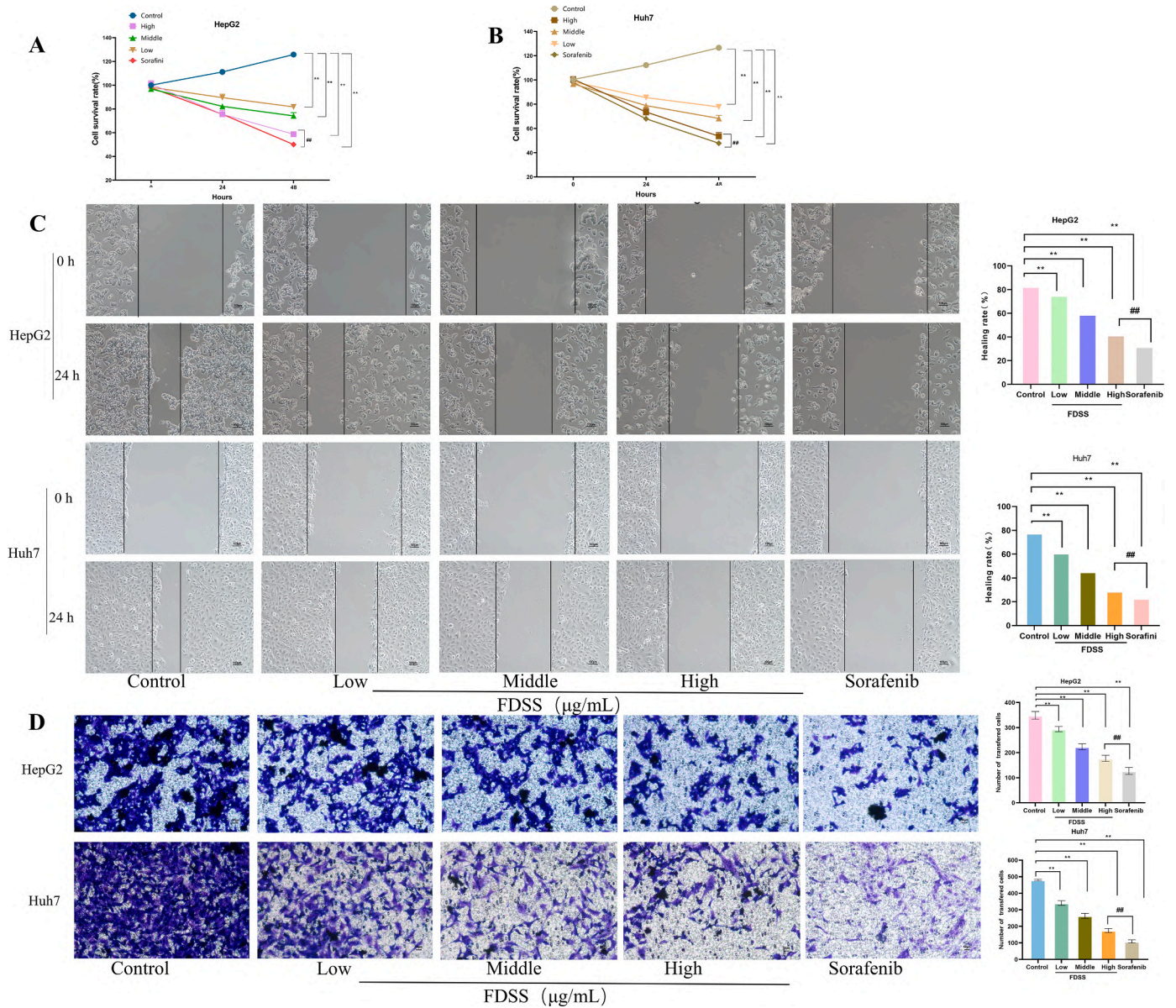


Fig. 2. FDSS inhibits HepG2 and Huh7 cell proliferation, migration, and invasion *in vitro*. (A, B) The cell viability of HepG2 and Huh7 cells treated with FDSS at indicated concentrations for 24 and 48 h by CCK-8 assay. (C) Migration of HepG2 and Huh7 cells treated with FDSS at indicated concentrations for 24 h by wound healing assay (100 × magnification). (D) Invasion of HepG2 and Huh7 cells treated with FDSS at indicated concentrations by transwell assay (200 × magnification). The data of all assays are shown as mean ± SD of three independent experiments. ### $P > 0.01$ and ** $P < 0.01$ for the designated treatment vs. control.

recurrence metastasis tendency, and poor prognosis. In the sorafenib group, a small number of tumor cells and the tumor cells increased in volume and Rnp. In the FDSS (5, 10, 20 $\mu\text{g}/\text{mL}$) groups, fewer tumor cells were seen in the abdominal cavity, and the tumor cell Rnp as well as pathological nuclear division decreased in a dose-dependent manner. These results also suggest that the FDSS could significantly inhibit the proliferation of HepG2 cells and improve the abnormal morphology of HepG2 cells.

3.3. FDSS induces HCC cells apoptosis

The impact of FDSS on cell cycle distribution was assessed using flow cytometry (Fig. 4A). In comparison to the control group, which had 25.16% of cells in the G0/G1 phase, the percentage of HepG2 cells in the G0/G1 phase increased to 31.42%, 37.61%, 49.53%, and 48.21% following treatment with FDSS at concentrations of 20, 40, and 80 $\mu\text{g}/\text{mL}$, as well as sorafenib at 4 $\mu\text{g}/\text{mL}$. Similarly, when compared to the

control group, which had 24.48% of cells in the G0/G1 phase, the percentage of Huh7 cells in the G0/G1 phase increased to 30.18%, 37.35%, 42.78%, and 43.62% after treatment with FDSS at concentrations of 20, 40, and 80 $\mu\text{g}/\text{mL}$. Notably, the percentage of Huh7 cells in the G0/G1 phase following treatment with FDSS at a concentration of 80 $\mu\text{g}/\text{mL}$ was slightly lower than that of the sorafenib group (43.62%). These findings provide evidence that FDSS hinders the growth of both HepG2 and Huh7 cells by inducing cell cycle arrest at the G0/G1 phase.

Subsequently, we assessed the impact of FDSS on apoptosis in liver cancer cells using annexin V-FITC/PI staining. FDSS elicited a dose-dependent increase in apoptosis rates in HCC cells compared to the control group ($P < 0.01$). The apoptosis rates for HepG2 cells after treatment with FDSS at concentrations of 20, 40, and 80 $\mu\text{g}/\text{mL}$, as well as sorafenib at 4 $\mu\text{g}/\text{mL}$, were 4.12%, 13.18%, 24.09%, 41.00%, and 41.60%, respectively. Similarly, for Huh7 cells, the corresponding apoptosis rates were 3.17%, 9.75%, 17.88%, 25.17%, and 29.17% (Fig. 4B). Additionally, the number of apoptotic cells increased

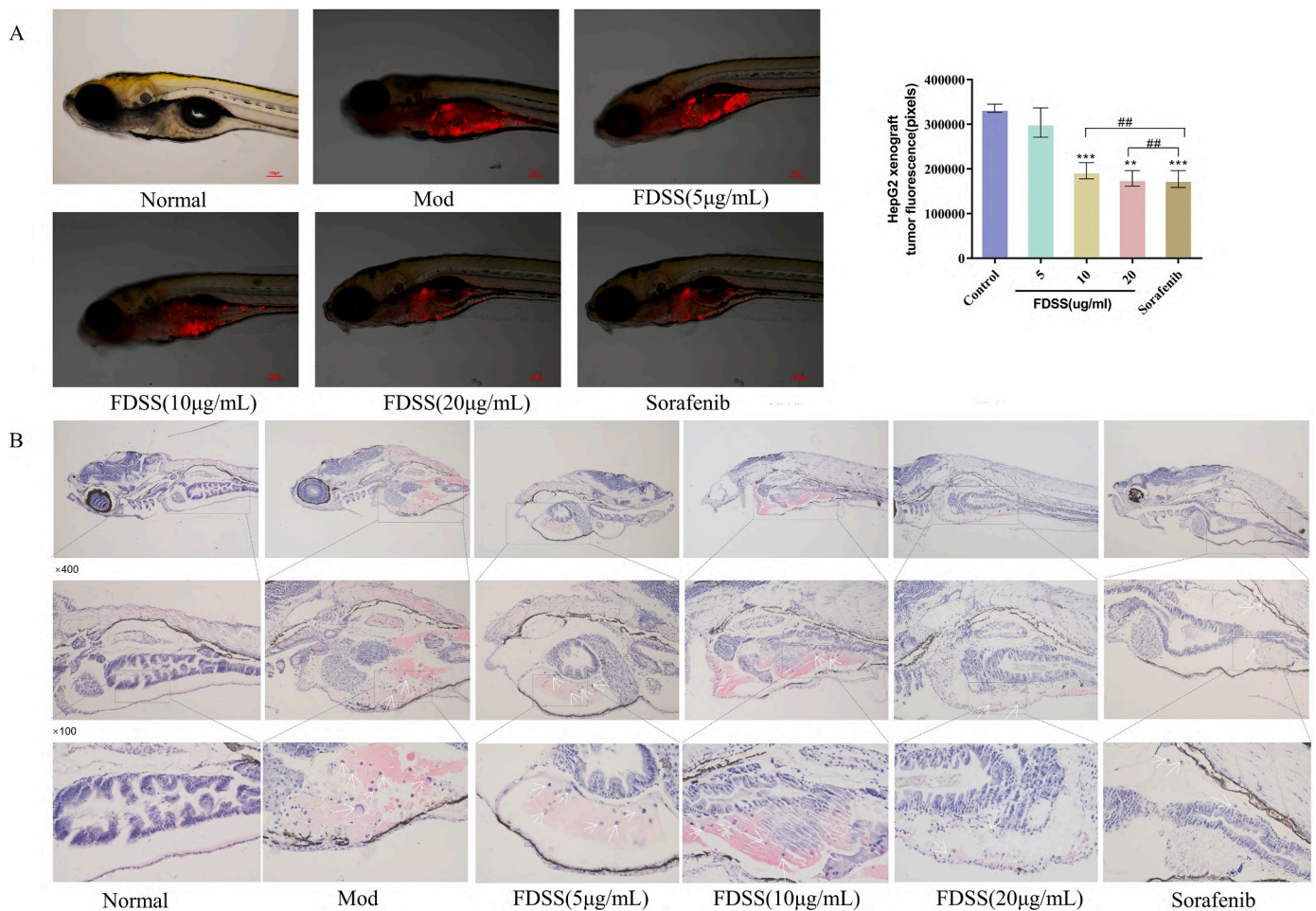


Fig. 3. FDSS inhibits HepG2 xenograft growth in zebrafish. (A) Tumor fluorescence values in HepG2 cells xenograft zebrafish after treatment with FFDS at indicated concentrations. * $P < 0.05$, ** $P < 0.01$, # $P > 0.05$, ## $P > 0.01$ compare with control group. (B) Histopathological structure of HepG2 xenograft zebrafish tumor models. The white arrow indicates the tumor cell.

significantly after treatment with FDSS at concentrations of 20, 40, and 80 $\mu\text{g}/\text{mL}$ compared to the control group ($P < 0.01$). The apoptotic effect of FDSS at a high concentration was comparable to that of the sorafenib group ($P > 0.01$). These findings highlight the pro-apoptotic potential of FDSS in liver cancer cells, particularly at higher concentrations.

TEM revealed the cellular morphology of HepG2 and Huh7 cells in the control group, displaying intact cell membranes with clearly visible nuclei and nuclear membranes (Fig. 4C). In the low-concentration group (20 $\mu\text{g}/\text{mL}$) and the moderate-concentration group (40 $\mu\text{g}/\text{mL}$) of Huh7 cells treated with FDSS, early signs of apoptosis were evident. These included wrinkling of the nuclear membrane and the formation of crescent-shaped nuclei clustered beneath the nuclear membrane. In the advanced stages of apoptosis, cell membranes exhibited further wrinkling, invagination, division, and envelopment of the cytoplasm. This process resulted in the formation of apoptotic bodies. Notably, in the high-concentration group (80 $\mu\text{g}/\text{mL}$) and the sorafenib-treated group (4 $\mu\text{g}/\text{mL}$), similar late-stage apoptotic changes were observed.

Interestingly, in the case of FDSS-treated HepG2 cells, only mitochondrial alterations were observed, characterized by mitochondrial swelling in the low and moderate concentration groups. At high concentrations in Huh7 cells, mitochondrial density decreased, and mitochondrial cristae became disrupted. These findings collectively suggest that FDSS treatment induces apoptosis in HCC cells and is associated with distinct morphological changes in mitochondria.

In the apoptosis assay conducted on xenograft tumor zebrafish (Fig. 4D), our observations revealed that, when compared to the model group, both the FDSS (10 $\mu\text{g}/\text{mL}$) group and the FDSS (20 $\mu\text{g}/\text{mL}$) group

significantly inhibited apoptotic fluorescence in HepG2 cells (all $P < 0.05$). Furthermore, there was no significant difference in tumor fluorescence between the FDSS (10 $\mu\text{g}/\text{mL}$) group and the sorafenib group ($P > 0.05$). Interestingly, the FDSS (20 $\mu\text{g}/\text{mL}$) group exhibited a higher level of tumor apoptotic fluorescence compared to the sorafenib group. These results provide clear evidence of FDSS's ability to induce apoptosis in HepG2 xenograft zebrafish.

3.4. FDSS inhibits HCC cells -induced angiogenesis

We investigated the effects of FDSS on tube formation by HUVECs induced by HepG2 or Huh7 cells using a co-culture assay (Fig. 5A). HUVECs co-cultured with HepG2 cells exhibited a significant increase in tube formation compared to HUVECs alone. However, HepG2 cells treated with FDSS (20, 40, 80 $\mu\text{g}/\text{mL}$) effectively suppressed the tube formation of HUVECs. Furthermore, FDSS inhibited the tube formation of HUVECs co-cultured with Huh7 cells. These findings strongly suggest that FDSS has the potential to inhibit angiogenesis induced by HCC cells.

We subsequently examined the impact of FDSS on tumor-induced angiogenesis using zebrafish implanted with HepG2 cells (Fig. 5B). Normally, the intestinal blood vessels of zebrafish display a continuous contour without any extravascular buds, and new blood vessel sprouting is primarily induced by tumors (Guo et al., 2020). The neovascularization budding ratios for the control group, FDSS (20, 40, 80 $\mu\text{g}/\text{mL}$) groups, and the sorafenib group were 80%, 20%, 13%, 7%, and 13%, respectively. These results indicate that FDSS can significantly inhibit tumor-induced neovascularization in the HepG2 xenograft

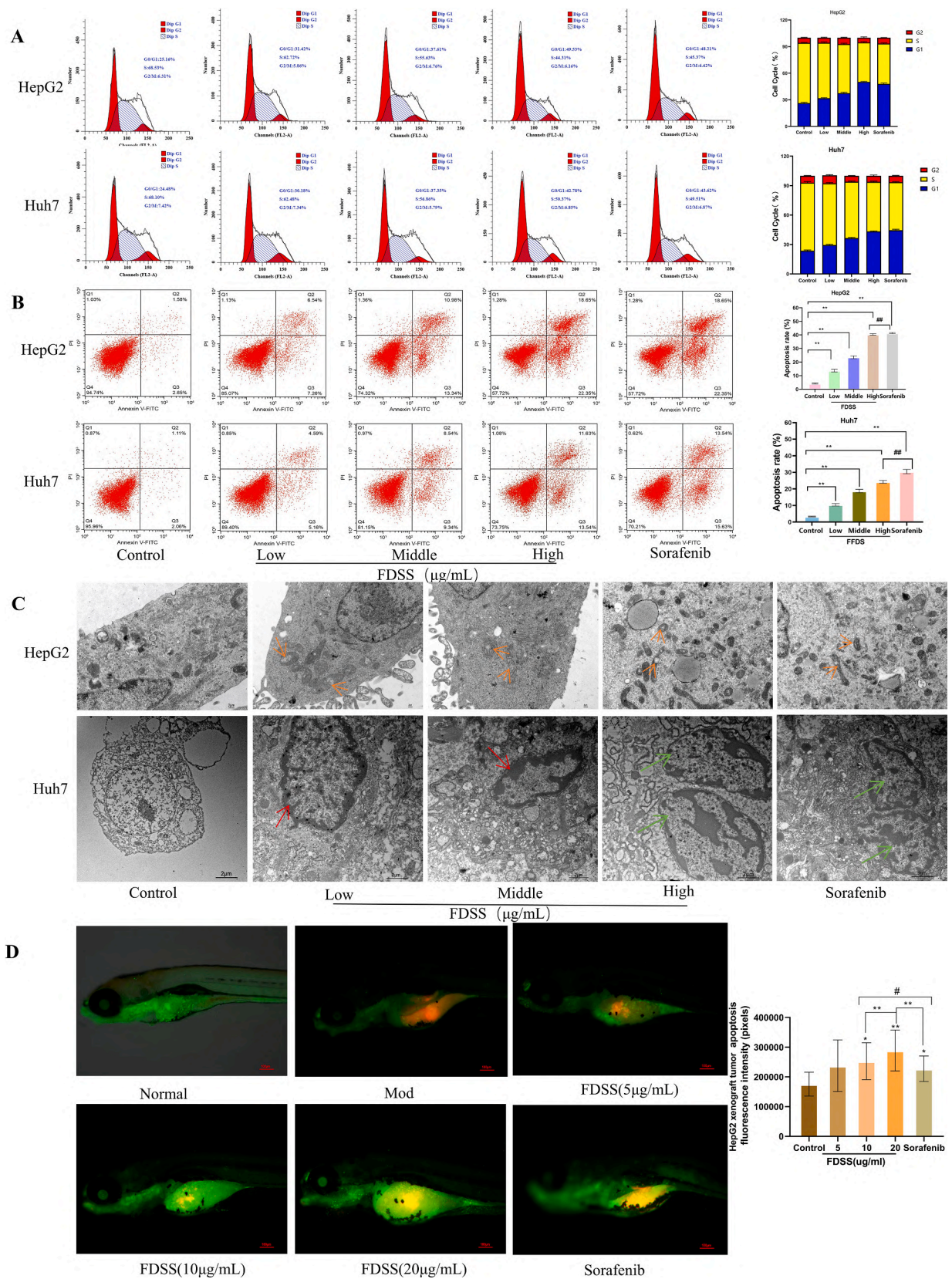


Fig. 4. The effects of FDSS on the HepG2 and Huh7 cell cycle and apoptosis. (A) Cell cycle of HepG2 and Huh7 cells treated with FDSS at indicated concentrations by flow cytometry. (B) Apoptosis of HepG2 and Huh7 cells treated with FDSS at indicated concentrations by annexin V-FITC and propidium iodide (PI) dual-labeling. (C) TEM image of HepG2 ($\times 8000$ magnification) and Huh7 ($\times 7000$ magnification) cells. The orange arrow indicates swollen mitochondria. The red arrow indicates crescent-shaped nuclei under the nuclear membrane. The green arrow indicates an apoptotic body. (D) Tumor apoptotic fluorescence changes in HepG2 cells xenograft zebrafish after treatment with FDSS at indicated concentrations. $*P < 0.05$, $**P < 0.01$, $\#P > 0.05$, $\#\#P > 0.01$ compare with control group.

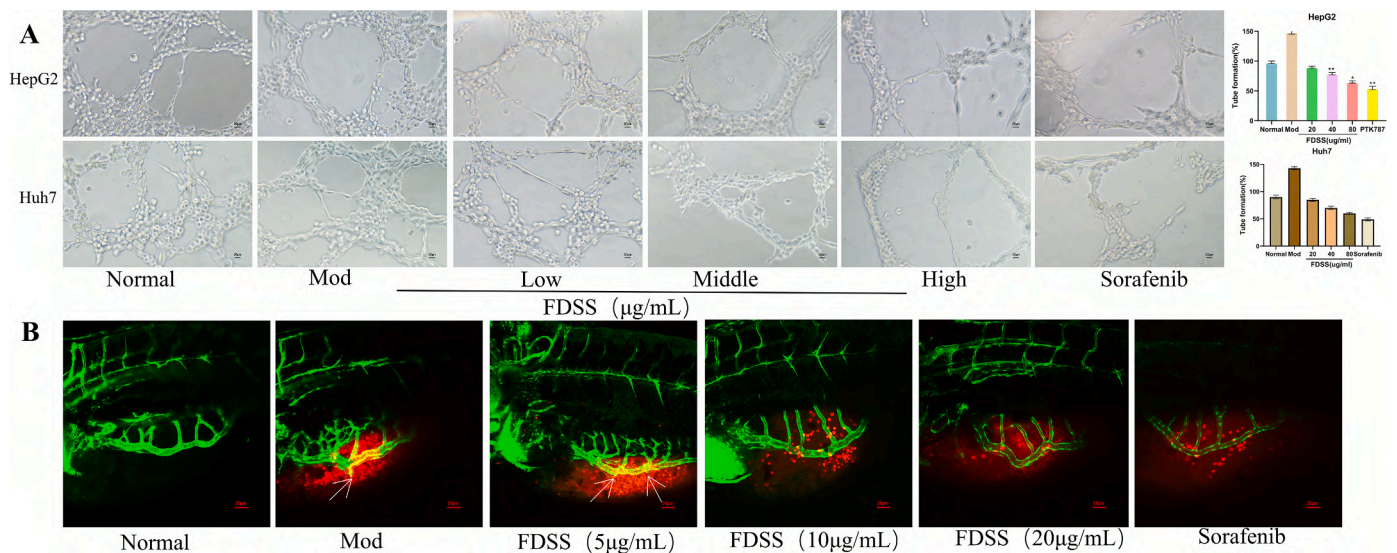


Fig. 5. FDSS inhibited cells-induced angiogenesis *in vitro* and *in vivo*. (A) HUVECs co-cultured with HepG2 and Huh7 cells, treated with FDSS at indicated concentrations. (B) Tumor-induced angiogenesis in zebrafish treated with FDSS at indicated concentrations (200 × magnification). Red represents HepG2 cells. White arrows point to tumor-induced neovascularization. ** $P < 0.01$, * $P < 0.05$, compared with model group

zebrafish model.

3.5. FDSS inhibits the expression of VEGFR and c-met proteins and promotes apoptotic proteins in HCC

We conducted a Western blot analysis to investigate whether the VEGFR and c-Met/apoptosis pathways play a role in regulating the anti-HCC activity of FDSS. In HepG2 cells and HepG2 xenograft tumor zebrafish, the expression of p-Met, p-AKT, and Bcl-2 proteins was downregulated, while the expression of Bax, caspase-9, and caspase-3 proteins were upregulated (Fig. 6 A, B).

To further confirm the impact of FDSS on the inhibition of c-Met and VEGFR activation, we treated HepG2 cells with HY-132814 (a c-Met agonist) or HY-N0545 (a VEGFR agonist) and observed an increase in the expression of c-Met and VEGFR compared to the HY-132814+FDSS

group and the control group ($P < 0.05$) (Fig. 6 C-F). This effect was reversed when SU11274 (a c-Met inhibitor) or sorafenib (a VEGFR inhibitor) was used. These findings indicate that FDSS may have a potential targeted effect on inhibiting the activation of c-Met and VEGFR, thus exhibiting anti-HCC properties.

4. Discussion

In order to substantiate the anti-tumor properties of FDSS, we conducted CCK-8 assays, transwell assays, and wound healing assays. Our findings revealed a substantial and dose-dependent decrease in the survival rate of HepG2 cells when exposed to FDSS, thus confirming previous results by Xiao, which demonstrated the inhibitory effects of SS extracts on HepG2 cell growth (Xiao et al., 2016). To comprehensively evaluate the impact of FDSS on HCC inhibition, we employed both in

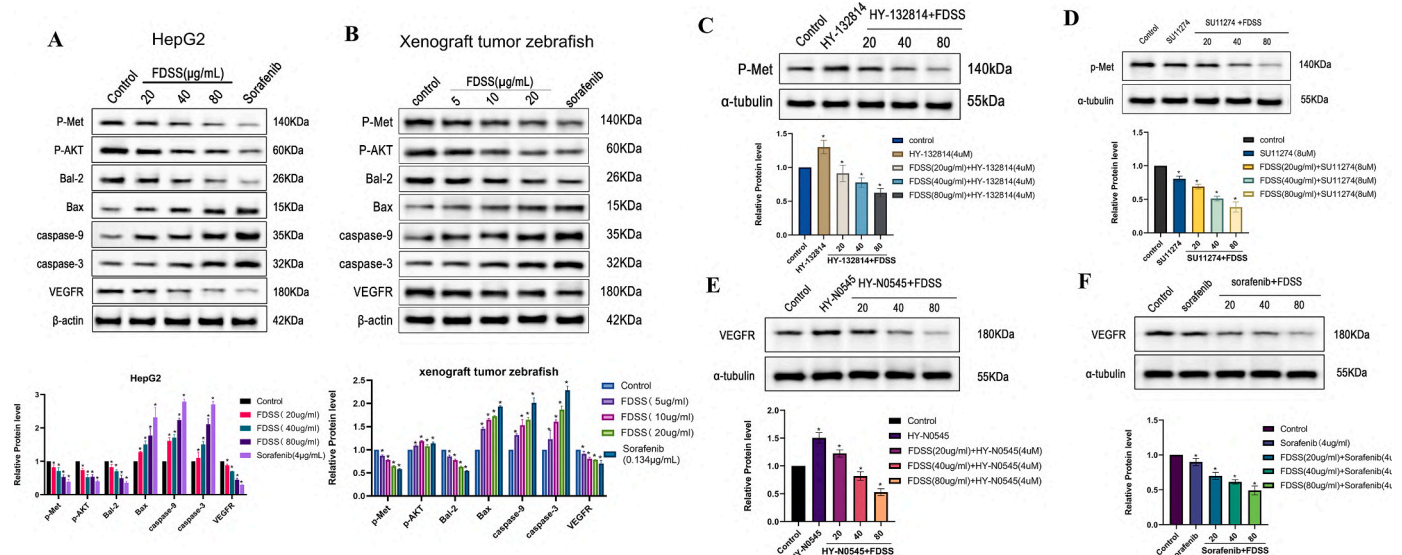


Fig. 6. Expression of VEGFR and c-Met/apoptosis pathway relative proteins and potential target effect of FDSS in HCC cells treated with FDSS. (A, B) Western blot analysis of p-Met, p-AKT, Bcl-2, Bax, caspase-9, caspase-3, and VEGFR expression in HepG2 cells and xenograft tumor zebrafish treated with FDSS. (C, D) The p-Met protein levels in HepG2 cells intervened with HY-132814 (c-Met agonist) and SU11274 (c-Met inhibitor) and treated with HY-132814+FDSS and SU11274+FDSS. (E, F) The VEGFR protein levels in HepG2 cells were intervened with HY-N0545 (VEGFR agonist) and sorafenib (VEGFR inhibitor) and treated with HY-N0545+FDSS and sorafenib + FDSS. The data represent the mean ± SD of three independent experiments. * $P < 0.05$.

vitro (Huh7 cells) and in vivo (xenograft zebrafish) models for further research. The results consistently showed that FDSS exerted significant inhibitory effects on both Huh7 cells and HepG2 xenograft tumor zebrafish. Moreover, there was a clear dose-dependent relationship between the treatment dose of FDSS and the suppression of p-Met expression, further underscoring its effectiveness in mitigating HCC.

Apoptosis is considered a good option for HCC treatment (Yang et al., 2022). Cell cycle assay, apoptosis assay, xenograft tumor zebrafish apoptosis assay, and TEM observation were performed to demonstrate the anti-HCC effects of FDSS. We found that FDSS arrests the cell cycle at the G0/G1 phase and increases apoptosis in HepG2 and Huh7 cells. FDSS also significantly inhibited the apoptotic fluorescence of xenograft tumor zebrafish. Recent studies show that c-Met can directly activate the apoptotic pathway (Kim et al., 2020). In this research, we uncovered a novel finding that FDSS effectively down-regulates Bcl-2 expression levels, while upregulating Bax, caspase-9, and caspase-3 expression levels. This modulation occurs through the intricate regulation of the c-Met pathway, ultimately resulting in the inhibition of HCC cell proliferation.

Evidence is mounting that neovascularization is essential for HCC proliferation, metastasis, and drug resistance (Morse et al., 2019). Inhibition of neovascularization is nowadays regarded as a new target for HCC therapy. Therefore, targeting VEGFR may be an effective method to inhibit HCC neovascularization. In this experiment, HUVECs were co-cultured with HepG2 and Huh7 cells, respectively, and HepG2 cells were implanted in vascular fluorescence zebrafish to observe the relationship between neovascularization and tumors. The findings demonstrated that FDSS significantly inhibited tumor-induced neovascularization by reducing VEGFR expression, which was modulated through the c-Met pathway.

In conclusion, FDSS shows promising potential as a treatment for HCC, with a mechanism of action involving the targeting of c-Met and VEGFR. Future studies should consider employing gene editing technologies to confirm the inhibitory effects of FDSS on the activation of c-Met and VEGFR in animal models. Ultimately, our research on FDSS offers valuable insights that could serve as a theoretical foundation for the development of effective targeted therapies and drug screening methods for HCC.

Consent for publication

Not applicable.

Availability of data and materials

The datasets used and analyzed during the current study are available from the corresponding author on reasonable request.

Ethics approval

The animal study was reviewed and approved by Ethics Committee of College of Traditional Chinese Medicine, Inner Mongolia Medical College. (No. SYXK (Zhe) 2022-000).

CRediT authorship contribution statement

Zhao-Hua Xu: Conceptualization. **Ying Dang:** Writing – original draft. **Yu Dong:** Writing – review & editing. **Chong-Yang Dong:** Formal analysis. **Yu Liu:** Writing – review & editing. **Xu Chen:** Writing – review & editing. **Zhi Yao:** Writing – review & editing. **Jian-Ping Shi:** Investigation.

Declaration of competing interest

The authors declare that they have no known competing financial interests or personal relationships that could have appeared to influence

the work reported in this paper.

Data availability

The data that has been used is confidential.

Acknowledgements

We thank the Inner Mongolia Natural Science Foundation of China (No. 2022SHZR0236) for funding.

Abbreviations

SS	Sorbaria sorbifolia
FDSS	Freeze-Dried powder of the water extract of <i>Sorbaria sorbifolia</i>
TCM	Traditional Chinese medicine
HUVECs	Human Umbilical Vein Endothelial Cells
HCC	Hepatocellular Carcinoma
VEGFR	Vascular Endothelial Growth Factor Receptor
TEM	Transmission electron microscopy
dpf	days post fertilization
Rnp	

References

- College, B.M., 2006. Medicine for promoting blood circulation and removing blood stasis. *Chin. J. Integr. Med.* 2105–2106. <https://doi.org/10.1007/s11655-020-3271-8> (in Chinese).
- Guo, Y., Fan, Y., Pei, X., 2020. Fangjihuangqi Decoction inhibits MDA-MB-231 cell invasion in vitro and decreases tumor growth and metastasis in triple-negative breast cancer xenografts tumor zebrafish model. *Cancer Med.* 9 (7), 2564–2578. <https://doi.org/10.1002/cam4.2894>.
- Jain, R.K., 2005. Normalization of tumor vasculature: an emerging concept in antiangiogenic therapy. *Science* 307 (5706), 58–62. <https://doi.org/10.1126/science.1104819>.
- Jang, J., Lee, J.S., Jang, Y.J., Choung, E.S., Li, W.Y., Lee, S.W., Kim, E., Kim, J.H., Cho, J. Y., 2020. Sorbaria kirilowii ethanol extract exerts anti-inflammatory effects in vitro and in vivo by targeting src/nuclear factor (NF)- κ B. *Biomolecules* 10 (5). <https://doi.org/10.3390/biom10050741>.
- Karmacharya, U., Guragain, D., Chaudhary, P., Jee, J.G., Kim, J.A., Jeong, B.S., 2021. Novel pyridine bioisostere of cabozantinib as a potent c-met kinase inhibitor: synthesis and anti-tumor activity against hepatocellular carcinoma. *Int. J. Mol. Sci.* 22 (18) <https://doi.org/10.3390/ijms22189685>.
- Kim, S.M., Han, J.M., Le, T.T., Sohng, J.K., Jung, H.J., 2020. Anticancer and antiangiogenic activities of novel α -mangostin glycosides in human hepatocellular carcinoma cells via downregulation of c-met and HIF-1 α . *Int. J. Mol. Sci.* 21 (11) <https://doi.org/10.3390/ijms21114043>.
- Kummar, S., Srivastava, A.K., Navas, T., Cecchi, F., Lee, Y.H., Bottaro, D.P., Park, S.R., Do, K.T., Jeong, W., Johnson, B.C., Voth, A.R., Rubinstein, L., Wright, J.J., Parchment, R.E., Doroshow, J.H., Chen, A.P., 2021. Combination therapy with pazopanib and tivantinib modulates VEGF and c-MET levels in refractory advanced solid tumors. *Invest. N. Drugs* 39 (6), 1577–1586. <https://doi.org/10.1007/s10637-021-01138-x>.
- Li, Y., Bian, L., Cui, F., Li, L., Zhang, X., 2011. TTF1-induced apoptosis of HepG-2 cells through a mitochondrial pathway. *Oncol. Rep.* 26 (3), 651–657. <https://doi.org/10.3892/or.2011.1330>.
- Li, Y., Liu, A., Wang, Y., Yan, X., 2013. The efficacy study on si ni san freeze-dried powder on sleep phase in insomniac and normal rats. *Evid Based Complement Alternat Med : eCAM* 2013, 947075. <https://doi.org/10.1155/2013/947075>.
- Liu, C., Li, X.W., Cui, L.M., Li, L.C., Chen, L.Y., Zhang, X.W., 2011. Inhibition of tumor angiogenesis by TTF1 from extract of herbal medicine. *World J. Gastroenterol.* 17 (44), 4875–4882. <https://doi.org/10.3748/wjg.v17.i44.4875>.
- Liu, Z., Ma, H., Lai, Z., 2023. The role of ferroptosis and cuproptosis in curcumin against hepatocellular carcinoma. *Molecules* 28 (4). <https://doi.org/10.3390/molecules28041623>.
- Luo, J., Chen, Q.X., Li, P., Yu, H., Yu, L., Lu, J.L., Yin, H.Z., Huang, B.J., Zhang, S.J., 2024. Lobelia chinensis Lour inhibits the progression of hepatocellular carcinoma via the regulation of the PTEN/AKT signaling pathway in vivo and in vitro. *J ethnopharmacology* 318 (Pt A), 116886. <https://doi.org/10.1016/j.jep.2023.116886>.
- Mahnashi, M.H., Ayaz, M., Alqahtani, Y.S., Alyami, B.A., Shahid, M., Alqahtani, O., Kabrah, S.M., Zeb, A., Ullah, F., Sadiq, A., 2023. Quantitative-HPLC-DAD polyphenols analysis, anxiolytic and cognition enhancing potentials of Sorbaria tomentosa Lindl. *Rehder. J ethnopharmacology* 317, 116786. <https://doi.org/10.1016/j.jep.2023.116786>.
- Morse, M.A., Sun, W., Kim, R., He, A.R., Abada, P.B., Mynderse, M., Finn, R.S., 2019. The role of angiogenesis in hepatocellular carcinoma. *Clin. Cancer Res.* 25 (3), 912–920. <https://doi.org/10.1158/1078-0432>.

- Qiu, G., Jin, Z., Chen, X., Huang, J., 2020. Interpretation of guidelines for the diagnosis and treatment of primary liver cancer (2019 edition) in China. *Glob Health Med* 2 (5), 306–311. <https://doi.org/10.35772/ghm.2020.01051>.
- Shoja, M.M., Tubbs, R.S., Shokouhi, G., Loukas, M., 2010. Wang Qingren and the 19th century Chinese doctrine of the bloodless heart. *Int. J. Cardiol.* 145 (2), 305–306. <https://doi.org/10.1016/j.ijcard.2009.10.042>.
- Siegel, R.L., Miller, K.D., Jemal, A., 2019. Cancer statistics, 2019. *CA Cancer J Clin* 69 (1), 7–34. <https://doi.org/10.3322/caac.21551>.
- Wang, H., Rao, B., Lou, J., Li, J., Liu, Z., Li, A., Cui, G., Ren, Z., Yu, Z., 2020. The function of the HGF/c-Met Axis in hepatocellular carcinoma. *Front. Cell Dev. Biol.* 8, 55. <https://doi.org/10.3389/fcell.2020.00055>.
- Wang, Z., Yu, X.L., Zhang, J., Cheng, Z.G., Han, Z.Y., Liu, F.Y., Dou, J.P., Kong, Y., Dong, X.J., Zhao, Q.X., Yu, J., Liang, P., Tang, W.Z., 2021. Huaier granule prevents the recurrence of early-stage hepatocellular carcinoma after thermal ablation: a cohort study. *J. ethnopharmacology* 281, 114539. <https://doi.org/10.1016/j.jep.2021.114539>.
- Wen, N., Cai, Y., Li, F., Ye, H., Tang, W., Song, P., Cheng, N., 2022. The clinical management of hepatocellular carcinoma worldwide: a concise review and comparison of current guidelines: 2022 update. *Biosci Trends* 16 (1), 20–30. <https://doi.org/10.5582/bst.2022.01061>.
- Xiao, B., Lin, D., Zhang, X., Zhang, M., Zhang, X., 2016. TTF1, in the form of nanoparticles, inhibits angiogenesis, cell migration and cell invasion in vitro and in vivo in human hepatoma through STAT3 regulation. *Molecules* 21 (11). <https://doi.org/10.3390/molecules21111507>.
- Yang, Z., Zhang, H., Yin, M., Cheng, Z., Jiang, P., Feng, M., Liao, B., Liu, Z., 2022. Neurotrophin3 promotes hepatocellular carcinoma apoptosis through the JNK and P38 MAPK pathways. *Int. J. Biol. Sci.* (15), 5963–5977. <https://doi.org/10.7150/ijbs.72982>.
- Ying Zhang, H.L., 2021. Quality control study of pearl plum based on fingerprinting combined with chemical pattern recognition. *J. Chin. Med. Mater.* 44, 636–640. <https://doi.org/10.13863/j.issn1001-4454.2021.03.024>.
- Zeng, H., Chen, W., Zheng, R., Zhang, S., Ji, J.S., Zou, X., Xia, C., Sun, K., Yang, Z., Li, H., Wang, N., Han, R., Liu, S., Li, H., Mu, H., He, Y., Xu, Y., Fu, Z., Zhou, Y., Jiang, J., Yang, Y., Chen, J., Wei, K., Fan, D., Wang, J., Fu, F., Zhao, D., Song, G., Chen, J., Jiang, C., Zhou, X., Gu, X., Jin, F., Li, Q., Li, Y., Wu, T., Yan, C., Dong, J., Hua, Z., Baade, P., Bray, F., Jemal, A., Yu, X.Q., He, J., 2018. Changing cancer survival in China during 2003–15: a pooled analysis of 17 population-based cancer registries. *Lancet Global Health* 6 (5), e555–e567. [https://doi.org/10.1016/S2214-109X\(18\)30127-X](https://doi.org/10.1016/S2214-109X(18)30127-X).
- Zhang, D.Q., Mu, Y.P., Xu, Y., Chen, J.M., Liu, P., Liu, W., 2022. Research progress in Chinese medicine preparations for promoting blood circulation and removing blood stasis for cirrhotic patients with portal vein thrombosis following splenectomy. *Chin. J. Integr. Med.* 28 (9), 855–863. <https://doi.org/10.1007/s11655-020-3271-8>.
- Zhang, X., Zhang, Y., Guan, L., Quan, Y., Sun, Q., 2004. [Study on extraction and isolation of active constituents from *Sorbaria sorbifolia* and antitumor effect of the constituents in vivo]. *Zhong yao cai = Zhongyao cai = Journal of Chinese medicinal materials* 27 (1), 36–38. <https://doi.org/10.13863/j.issn1001-4454.2021.03.024>.
- Zhang, X.W., Cui, C.X., Chen, L.Y., 2007. [Inhibition of *Sorbaria sorbifolia* on proliferation of hepatoma HepG-2 cell line]. *Zhong yao cai = Zhongyao cai = Journal of Chinese medicinal materials* 30 (6), 681–684. <https://doi.org/10.13863/j.issn1001-4454.2007.06.027>.